Supplement of

Sea ice and productivity changes over the last glacial cycle in the Adélie Land region, East Antarctica, based on diatom assemblage variability

Lea Pesjak et al. 2021

Correspondence to Lea Pesjak (lea.pesjak@utas.edu.au)

Table S1 Environmental interpretation of diatom species identified within Tan_44, based on water column and sediment studies from coastal Antarctica to Subantarctic Southern Ocean. The three species types identified by both types of studies include: sea ice associated species (blue), open ocean associated species (yellow), and warmer water associated species (orange; Medlin and Priddle 1990). This list includes *Eucampia antarctica* Terminal/Intercalary valve ratio. This list suggests there are some differences in interpretation of species habitat depending on the type of study conducted. Reference notes are: 1) Medlin and Priddle (1990); 2) Ligowski, Godlewski and Lukowski (1992); 3) Garrison and Buck (1989); 4) Kopczynska, Weber and El-Sayed (1986); 5) Tanimura et al. (1990); 6) Scott and Thomas (2005); 7) Kopczyńska, Fiala and Jeandel (1998); 8) Ligowski (1983); 9) Garrison, Buck and Fryxell (1987); 10) Beans et al. (2008); 11) Fryxell (1991); 12) Moisan and Fryxell (1993); 13) Doucette and Fryxell (1985); 14) Johansen and Fryxell (1985); 15) Smetacek et al. (1992); 16) Bodungen et al. (1986); 17) Smith and Nelson (1986); 18) Ishikawa et al. (2001); 19) Pichon et al. (1992); 20) Armand et al. (2005); 21) Romero et al. (2005); 22) Zielinski and Gersonde (1997); 23) Kaczmarska et al. (1993); 24) Leventer (1992); 25) Taylor, McMinn and Franklin (1997); 26) Crosta et al. (2005).

W	S	Species/ ratio	ENIRONMENTAL INTERPRETATION WATER COLUMN AND SEA ICE STUDIES	SEDIMENT SURFACE STUDIES
op	si	*Actinocyclus actinochilus* (Ehrenberg) Simonsen	Sea ice edge; rare in ice; coastal [1, 2, 3]	Sea ice >7 months/yr; sea ice edge; along ice shelves [19, 20]
w	w	*Azpeitia tabularis*	Subantarctic, rare near sea ice [1]	Open ocean, warmer water; north of Polar Front [21,22]
op	w	*Asteromphalus hyalinus* Karsten	Coastal, north and south of Polar Front [4, 5, 6]	Open ocean, warmer water; north of Polar Front [21]
op	w	*Asteromphalus parvulus* Karsten	Coastal; north and south of Polar Front [4, 6]	Open ocean, warmer water; north of Polar Front [21]
op		*Chaetoceros bulbosum* (Ehrenberg) Heiden	Open ocean; south of Polar Front; rare in ice [7, 3]	
op		*Chaetoceros dichaeta* (Ehrenberg)	Open ocean; sea ice; south of Polar Front [8, 9, 4, 7]	
op	op	*Eucampia antarctica* (Castracane) Mangin	Open ocean; south of Polar Front; rare in sea ice [3, 10]	Coastal to Subtropical Front; increases in glacial intervals [22, 23]
si	si	***Eucampia antarctica* Terminal/ Intercalary ratio**	Higher ratio indicates Winter stage (Prydz Bay) [11]	Sea ice; along ice shelves (Ross Sea) [19]
op	op	*Fragilariopsis kerguelensis*	Open ocean; south of Polar Front; rare in sea ice; increases offshore [4,3,7]	Open ocean; increases seaward; winter sea ice edge; Polar Front [20,22,24]
op	si	*Fragilariopsis angulata*	Open ocean [1]	Sea ice; coastal [25]
si	si	*Fragilariopsis cylindrus*	Sea ice; sea ice edge; open ocean; coastal; winter sea ice edge [9,12,2]	Sea ice >7 months/yr; coastal [20, 22]
si	si	*Fragilariopsis linearis*	Sea ice; ice edge [1,12]	Sea ice; along ice shelves [19, 20]
si	si	*Fragilariopsis obliquecostata*	Sea ice [3]	Sea ice >7 months/ yr; sea ice edge [20]
si	si	*Fragilariopsis sublinearis*	Sea ice; sea ice edge [1,12]	Sea ice >7 months/ yr [19,20]
op	op	*Rhizosolenia antennata*	Open ocean [10]	Open ocean; cooler water; sea ice edge [26]
op	op	*Rhizosolenia styliformis* Brightwell	Open ocean; south of 62°S/ south of Polar Front; rare in sea ice [4,3]	Open ocean; cooler water; sea ice edge [26]
op	op	*Thalassiosira lentiginosa* (Janish) Fryxell	Open ocean; south of the Polar Front [14]	Open ocean; 0-7°C; between winter sea ice edge and Polar Front; coastal [26,22,25]
op	op	*Thalassiosira oliverana*	Open ocean; antarctic and subantarctic [1]	Open ocean; between winter sea ice edge to Polar Front [26]
op	si	*Thalassiosira tumida* (Janish) Hasle	Open ocean; ice edge; sea ice; coastal; common south of Polar Front [3,17,18,14]	Sea ice >8.5 months/yr [20]
op	op	*Thalassiothrix antarctica*	Open ocean; coastal; sea ice edge; south of Polar Front [2,10,8,7]	Open ocean; diatom ooze belt [19,26]
op	op	*Thalassiothrix longissima* Cleve and Grunow	Open ocean; rare in sea ice [3]	Open ocean [26]
op	op	*Trichotoxon reinboldii*	Open ocean [1]	Open ocean; cooler water; south of Polar Front [26,25]

W interpretation based on water column studies

S interpretation based on sediment surface studies

si sea ice related species

op open ocean; sea ice edge

w north of Polar Front (warmer)

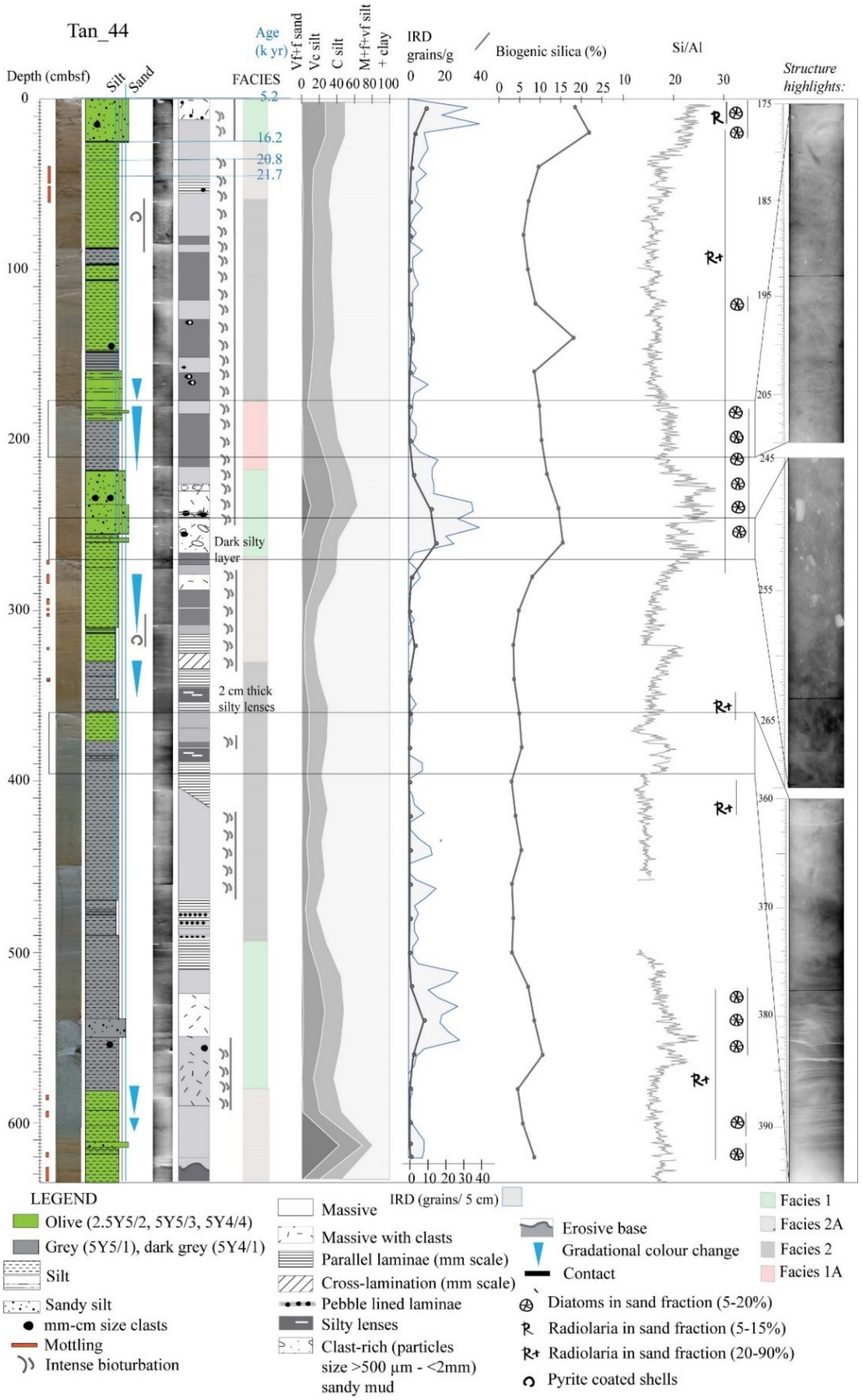

Figure S1 Lithology, structure, grain size, biogenic silica, ice rafted debris (IRD) counted from sieved sections (grains/g) and from X-radiographs (grains/ 5 cm), Si/Al (XRF-derived), and diatom and radiolaria estimates of the sand fraction (symbols). Included in this figure is the facies interpretation of core Tan_44. The facies model is based upon primary lithology identified in core logs (olive sandy mud; olive mud; grey mud; and olive-grey mud), Si/Al, biogenic silica and IRD results. Included are X-radiographs of parts of core.

S1 Development of the facies model

S1.1 Methods

Tan_44 lithology was described on the voyage (Williams 2013). The X-radiographs were completed at the National Institute of Water and Atmospheric Research (NIWA; Williams 2013). Sampling for grain size, biogenic silica, and ice rafted debris (IRD) were taken at 20 cm resolution down core. Sampling for diatom analysis were taken at 10 cm resolution within 350-0 cm interval. Microfossil and micropyrite estimates were completed using a binocular microscope, on a sieved sand (>63 µm) fraction.

S1.1.1 Grain Size

Grain size was determined using a Beckman Coulter 13320 laser diffraction particle size analyser. A sample size of 0.5 x 0.5 cm was soaked overnight in a mixture of sodium hydrogen carbonate, sodium carbonate (anhydrous) and water. The sediment in solution was then shaken and placed through a sonic bath for 10 second intervals, several times, to disaggregate clay. This sample was poured into the grain size analyser through a 1.8 mm sieve and analysed for 60 seconds, prior to a 3-minute cleaning routine. The grain size statistics were calculated using GradistatV8 software (Blott & Pye 2001), which uses the Folk and Ward method for size distribution and description.

S1.1.2 Ice Rafted Debris (IRD)

Ice rafted debris (IRD) analysis was completed using two methods, counting visible grains from X-radiographs (grains ≥1 mm, in 5 cm sections), and counting sieved grains (grains >500 µm; and dividing the number by weight, g). The size >500 µm, medium sand (Patterson et al. 2014) was chosen as the size that defines IRD because laser particle diffraction of samples showed the grain size <250 µm forms the matrix of all the samples. This is in contrast to other Antarctic studies, which defined IRD as >2 mm (Grobe et al. 1992; Diekmann et al. 2003), very coarse sand size, >1 mm (Lucchi et al. 2002; Pudsey & Camerlenghi 1998), >250 µm (Wilson et al. 2018), and >125 µm (Cook et al. 2013; Passchier 2011).

S1.1.3 X-ray fluorescence (XRF) data: Fe, Ti, Fe/Ti, Ba/Ti, Zr/Rb

The XRF methods are explained in main text.

S1.2 Results

Four lithological units are identified in Tan_44 (Fig. S1), based on visual logs (Williams 2013) and structural features identified in X-radiographs (Fig. S1). Unit 1 is olive sandy mud, comprising olive (2.5Y5/2, 5Y5/3), or grey colour (5Y4/1, 5Y5/1) within 581-493 cm section, and is characterised by a sandy texture, massive structure with dispersed >1 mm sized grains. Unit 2A is olive mud (2.5Y5/2; 5Y4/4) comprising a massive structure, bioturbation, and rare traction structures, i.e., lenses and laminae. Mottling is found at 46-37 cm; 58-54 cm; 584 cm, 594 cm, and 619 cm. Unit 2 is grey mud, comprising grey (5Y5/1) and olive (2.5Y5/2) colour, within section 147-59 cm and is characterised by a finer texture (than Unit 1). The younger Unit 2 (178-59 cm) contains a massive structure with evident bioturbation within the 147-59 cm section, while the older Unit 2 (493-331 cm) contains laminae and pebble-lined laminae. Gradation is observed at the base of the younger unit (at 178-159 cm), and within the lower unit (at 353-331 cm). Unit 1A is olive-grey mud (2.5Y 5/2) comprising a finer texture (than in Unit 1), with a massive structure and evident bioturbation.

Diatom and radiolaria species percentage were estimated for the sand fraction. The diatom estimates range from 0- ~20%, while the radiolaria estimates range from 0- ~97%, per sand fraction of the sample (Fig. S1). This interpretation is dependent on the total amount of the sand fraction per sample and is therefore only an estimate of surface productivity. Intervals with highest diatom estimates (5-10%) are found in olive sandy mud (Unit 1). Intervals with highest radiolaria estimates (20-80%) coincide with 280-0 cm (Unit 1; 1A; 2; 2A), and 620-520 cm (Unit 1, 2A) sections. Pyrite coated foraminifera and radiolaria shells, and some framboidal pyrite are found at 80-60 cm (Unit 2A), and at 320-300 cm (Unit 2A; Fig. S1).

S1.2.1 Grain size

A down core grain size pattern exists, formed by the alternation of coarser grained (sandy silt) and finer grained (silt) sediments (Fig. S1). The sandy silt intervals consist of 1-9% very fine to fine sand and, 19-27% very coarse silt. The silt intervals consist of increased medium silt to clay, up to 68% in the upper core, and up to 86% in the lower core. The sandy silt intervals coincide with higher Zr/Rb values and Unit 1. The silt intervals coincide with lower Zr/Rb, and Unit 2, Unit 2A and Unit 1A (Fig S1; Fig. S2).

S1.2.2 Ice rafted debris

High counts of ice rafted debris (IRD; 4-36 grains/5 cm) are found in Unit 1 (Fig. S1), with maximum counts found at 15-10 cm, at 255-250 cm and at 500-495 cm. Lower numbers of IRD (0-14 grains/5 cm) are found in Unit 2, Unit 2A and Unit 1A.

S1.2.3 X-ray fluorescence (XRF) data: Fe, Ti, Fe/Ti, Ba/Ti, Zr/Rb

Fe and Ti are generally parallel down core. Fe values range from ~23,000- ~44,000 counts per second (cps) and Ti values range from ~ 6,000-25,000 cps. Lower Fe values (~<33,000) are found in core sections 30-0 cm, 280-220 and 575-500 cm, which coincide with Unit 1 (Fig. S2). Similarly, lower Ti values occur in Unit 1. Fe/Ti values range from ~1.3- ~2.0, with lower values (<1.5) at 30-0 cm, 285-218 cm, and 580-500 cm, coinciding with Unit 1, and higher values (>1.5) coinciding with Unit 2 and Unit 2A.

Ba/Ti and Zr/Rb are generally parallel down core, aligned with Si/Al (Fig. S2), except within 255-230 cm (Unit 1) section where Ba/Ti decreases significantly. Ba/Ti values range from 0-0.06, with highest values (0-0.06) associated with Unit 1 and Unit 1A, and lower values (0-0.04) associated with Unit 2 and Unit 2A, and in the 255-230 cm section of Unit 1. Zr/Rb values range from 0.6-1.8, with highest values (~>1) associated with Unit 1 and Unit 1A, and lower values (~<1) associated with Unit 2 and Unit 2A, except in 331-328 cm section of Unit 2A, where slightly higher Zr/Rb values are found.

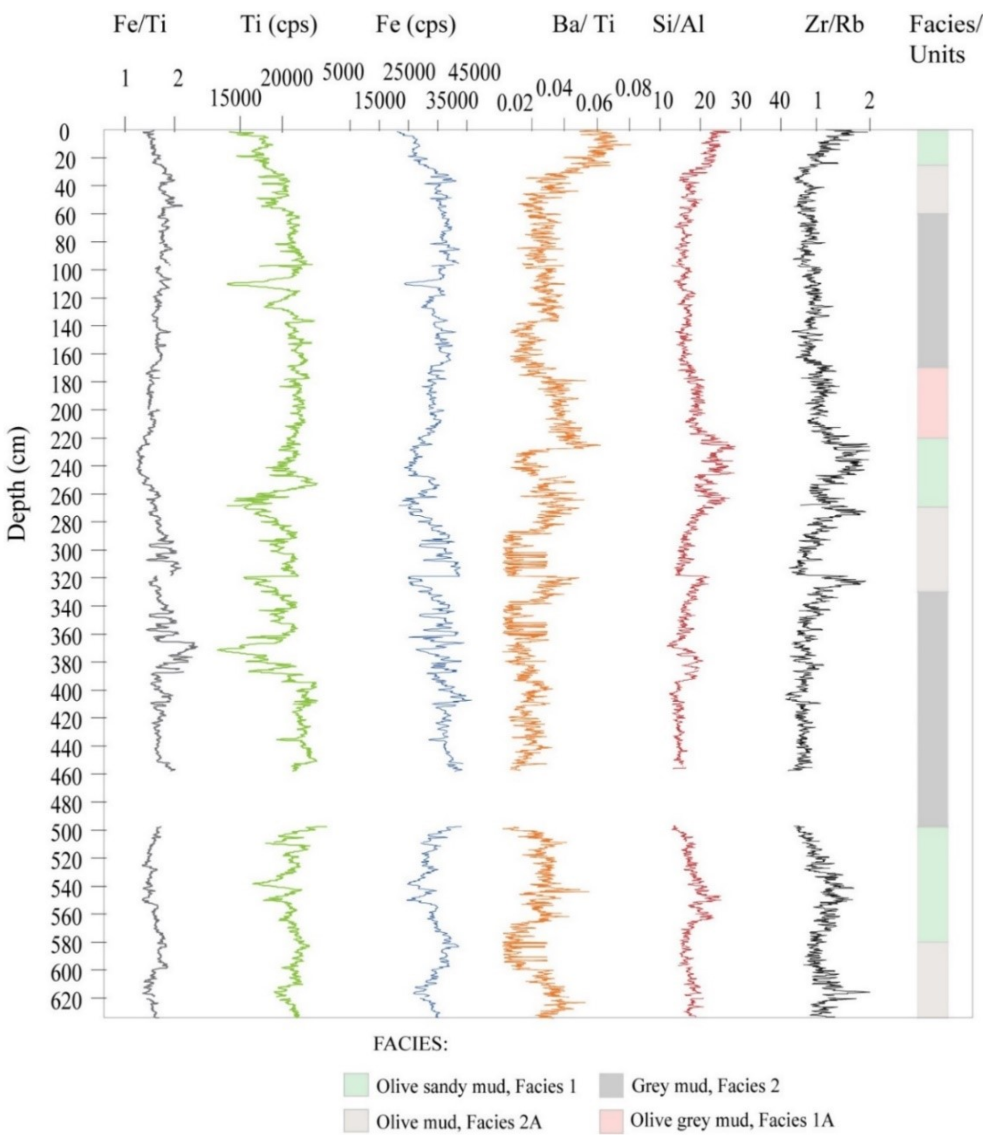

Figure S2 XRF data in Tan_44: Fe/Ti; Fe; Ti; Ba/Ti; Si/Al and Zr/Rb down core values, compared to glacial, interglacial, deglacial and glaciation facies occurrence.

Table S2 Radiocarbon dating (AIOM) conventional and calibrated results.

Lab No.	Sample	Depth (cm)	Conventional radiocarbon age (yr BP)	Error ± (yr)	δ 13C	Calibrated age (cal. yr BP); ΔR=830+/-200	Calibrated mean (yr BP)
OZV390	Tan44_0cm	0.5-3.5	5,765	45	-25	4,971-5,478	5,233
OZV391	Tan44_25cm	25.5-26.5	14,660	80	-23.6	15,837-16,468	16,160
OZV392	Tan44_35cm	35.5-36.5	18,470	90	-23.9	20,504-21,082	20,803
OZV393	Tan44_45cm	45.0-46.0	19,150	140	-25	21,340 - 22,007	21,682

Table S3 Q-mode principal component factor loadings of each principal component (assemblage; PC 1-4).

Species, group, ratio	Principal component			
	1	2	3	4
Thalassiosira lentiginosa	0.995	-0.046	-0.009	0.083
Azpeitia tabularis	0.591	-0.266	-0.011	0.235
Stellarima microtiras	0.014	0.000	0.078	-0.069
Actinocyclus ingens	-0.197	-0.288	0.746	0.142
Thalassiosira oliverana	0.033	0.294	0.560	-0.101
Eucampia antarctica	-0.878	-0.147	-0.052	-0.451
E antarctica T/I	-0.174	-0.401	0.089	0.096
Asteromphalus parvulus	0.147	0.692	-0.068	0.021
Asteromphalus hyalinus	0.548	0.217	-0.136	-0.072
Thalassiosira oestrupii	0.221	0.046	0.028	0.244
Fragilariopsis kerguelensis	0.143	0.052	-0.483	0.860
Actinocyclus actinochylus	-0.695	-0.110	0.594	-0.103
Thalassiothrix group	0.248	-0.215	0.015	0.433
Fragilariopsis group	-0.121	0.897	-0.087	0.191
Chaetoceros bulbosum	0.035	0.069	0.027	0.423
Rhizosolenia group	-0.344	0.674	-0.062	-0.031
Thalassiosira tumida	0.242	0.604	0.104	-0.074
Chaetoceros dichaeta	-0.083	0.512	0.165	0.109

Table S4 R-mode principal factor analysis: the main components (PC 1-4) loadings down core.

Depth (cm)	Component			
	PC1	PC2	PC3	PC4
5	0.929	0.084	0.353	0.034
20	0.632	0.376	0.67	-0.09
30	0.529	0.388	0.753	-0.045
40	0.599	0.28	0.736	0.125
50	0.139	0.5	0.855	0.027
60	0.306	0.708	0.609	-0.096
70	0.101	0.945	0.308	0.022
80	0.244	0.954	0.167	0.021
90	0.233	0.965	0.091	0.047
100	0.223	0.959	0.151	0.056
110	0.412	0.845	0.34	-0.005
120	0.156	0.876	0.457	-0.001
130	0.51	0.778	0.361	-0.005
140	0.408	0.825	0.388	-0.034
150	0.785	0.408	0.463	-0.016
160	0.823	0.497	0.253	0.077
170	0.615	0.701	0.31	0.169
180	0.891	0.347	0.203	0.178
190	0.796	0.486	0.348	0.01
200	0.692	0.532	0.46	0.081
210	0.583	0.678	0.148	0.415
220	0.531	0.438	0.653	0.31
230	0.787	0.299	0.535	-0.062
240	0.844	0.353	0.383	-0.085
250	0.978	0.154	0.111	-0.048
260	0.936	0.128	0.32	0.032
270	0.872	0.073	0.469	0.095
280	0.903	0.398	-0.12	0.084
290	0.81	0.566	0.146	-0.015

Table S5 List of diatom species in Tan_44, including terminal and intercalary valve counts of *Eucampia antarctica*.

DEPTH (cm)	5	20	30	40	50	60	70	80	90	100	110	120
Actinocyclus actinochylus	7	12	12	20	9	51	28	15	75	27	39	46
Actinocyclus ingens	1	1				45	7		4	2	2	4
Asteromphalus hookeri	5	5	3	6	8		1	3	1	2	1	1
Asteromphalus hyalinus	2	5	5	5	4		2					
Asteromphalus parvulus	4	3	3		3			1		3	1	1
Azpeitia tabularis	14	24	22	31	31				4	1	4	4
Chaetoceros bulbosum				10								
Chaetoceros chriophilus												
Chaetoceros adelianum				1								
Chaetoceros dichaeta												
Chaetoceros flexuosus												
Cocconeis costata												
Coscinodiscus asteromphalus		2									2	
Coscinodiscus bouvet				1		1						
Coscinodiscus curvatulus	1	6		2	5							
Coscinodiscus oculides			1	1			1		1			1
Coscinodiscus radiatus				1					1			
Coscinodiscus marginatus												
Coscinodiscus vulnificus		1						1	1			
Eucampia antarctica terminal valve	3	13	9	3	7	41	108	43	100	120	59	103
Eucampia antarctica intercalary valve	30	25	13	7	5	61	140	82	226	222	120	127
Eucampia antarctica	33	38	22	10	12	102	248	125	326	342	179	230
Fragilariopsis kerguelensis	42	8	27	83	87		4		12	13	6	9
Fragilariopsis obliquecostata	1								2		3	1
Fragilariopsis sublinearis	1	1									1	2
Fragilariopsis linearis												
Fragilariopsis angulata												
Fragilariopsis cylindrus												
Fragilariopsis curta												
Fragilariopsis vanheurckii												
Fragilariopsis seriata	1											
Fragilariopsis ritscherii									1			
Fragilariopsis babieri					1							
Fragilariopsis pseudoanana					1							
Porosira glacialis	2			1		1	1	2			1	
Porosira pseudodenticulata							2					
Rhizosolenia simplex				1				2		1		
Rhizosolenia polydactila												
Rhizosolenia sp.							1	1	1			
Rhizosolenia hebetata												
Rhizosolenia setigera							1					
Rhizosolenia antennata												
Rhizosolenia (twin process) antennata												1
Rhizosolenia inermis												
Rhizosolenia curvata												
Stellarima microtrias	3	2	1	1	0	6	1	0	8	5	7	3
Thalassiosira gracilis	2	1		1		1	3	1			4	
Thalassiosira lentiginosa	291	307	324	266	319	164	87	53	118	130	157	144
Thalassiosira oestrupii		2	9	13	12	1	2	2	3	1	3	1
Thalassiosira oliverana	25	24	9	6	12	26	9	4	17	15	10	17
Thalassiosira ritscherii	2				1	1						
Thalassiosira tumida	5	3	4	9	4		1	2	2	3	3	7
Thalassiotrix antarctica		2		11					1			
Thalassiothrix longisima	1				3							
Trichotoxon reinboldii			1	2	1							
Triceratium spp.												
Total counts	444	446	443	482	513	399	399	212	578	545	423	472

DEPTH (cm)	130	140	150	160	170	180	190	200	210	220	230	240
Actinocyclus actinochylus	46	37	26	29	32	17	24	35	29	20	19	31
Actinocyclus ingens	2	1	1							1		1
Asteromphalus hookeri	2	6	1	8	7	1		2			3	1
Asteromphalus hyalinus		3	16	7	11	1	7	4	3	1	4	9
Asteromphalus parvulus	4	4	1	6	10	6		10	2	2	6	6
Azpeitia tabularis	5		1	3			1	5	4	3	9	4
Chaetoceros bulbosum					4	1						1
Chaetoceros chriophilus					1			1				
Chaetoceros adelianum												
Chaetoceros dichaeta		2						20				
Chaetoceros flexuosus				2			1	4				
Cocconeis costata												2
Coscinodiscus asteromphalus						1					1	1
Coscinodiscus bouvet												
Coscinodiscus curvatulus				2	2	1	1	1				2
Coscinodiscus oculides		3			1	3			1			
Coscinodiscus radiatus												
Coscinodiscus marginatus										1		
Coscinodiscus vulnificus				1					1			
Eucampia antarctica terminal valve	42	58	20	19	35	8	22	20	35	14	11	17
Eucampia antarctica intercalary valve	102	111	65	104	125	73	92	73	163	32	34	79
Eucampia antarctica	144	169	85	123	160	81	114	93	198	46	45	96
Fragilariopsis kerguelensis	11		24	35	58	46	23	42	126	92	15	8
Fragilariopsis obliquecostata	2	1		26	28	31	31	32	7	6	3	5
Fragilariopsis sublinearis	2							1	3			
Fragilariopsis linearis										3		
Fragilariopsis angulata										2	1	
Fragilariopsis cylindrus												
Fragilariopsis curta												
Fragilariopsis vanheurckii												
Fragilariopsis seriata												
Fragilariopsis ritscherii												
Fragilariopsis babieri												
Fragilariopsis pseudoanana												
Porosira glacialis	1	1	1		1			2				
Porosira pseudodenticulata												
Rhizosolenia simplex	3	5	3	5	5	4	7	7	2	2	1	2
Rhizosolenia polydactila					1						1	
Rhizosolenia sp.		2										
Rhizosolenia hebetata					1							
Rhizosolenia setigera												
Rhizosolenia antennata					1							
Rhizosolenia (twin process) antennata				1	2			1	2	1	1	
Rhizosolenia inermis								1				
Rhizosolenia curvata		1										
Stellarima microtrias	5	2	3	3	6	5	6	3	0	0	0	1
Thalassiosira gracilis	2		3								1	4
Thalassiosira lentiginosa	162	164	284	227	194	180	249	202	179	165	293	325
Thalassiosira oestrupii	6	8		8	3	3	6	2	4	3	3	14
Thalassiosira oliverana	10	11	16	9	16	11	23	26	22	5	19	47
Thalassiosira ritscherii							1	4	1		1	
Thalassiosira tumida	7	1	3	12	11	5	10	12	3	3	10	23
Thalassiotrix antarctica												
Thalassiothrix longisima												
Trichotoxon reinboldii												
Triceratium spp												
Total counts	414	421	468	507	555	397	504	510	587	356	436	583

DEPTH (cm)	250	260	270	280	290	300	310	320	330	340	350
Actinocyclus actinochylus	15	34	3	31	37	5	9	1	1		
Actinocyclus ingens	1			13	7		12				
Asteromphalus hookeri	7	3	1	4	3		2				
Asteromphalus hyalinus	10	5	9	1	1		2				
Asteromphalus parvulus	2	1	3		1						
Azpeitia tabularis	20	27		2			1				
Chaetoceros bulbosum											
Chaetoceros chriophilus											
Chaetoceros adelianum											
Chaetoceros dichaeta											
Chaetoceros flexuosus											
Cocconeis costata	1										
Coscinodiscus asteromphalus		1		1			1				
Coscinodiscus bouvet											
Coscinodiscus curvatulus	1	8	1	1						1	1
Coscinodiscus oculides	1				2						
Coscinodiscus radiatus				1	2						
Coscinodiscus marginatus					2		2			1	
Coscinodiscus vulnificus											
Eucampia antarctica terminal valve		7	2		21	9	4	1			2
Eucampia antarctica intercalary valve	87	71	11	137	118	37	61	3	2	1	2
Eucampia antarctica	87	78	13	137	139	46	65	4	2	1	4
Fragilariopsis kerguelensis	9	63	74	28	8		10				
Fragilariopsis obliquecostata			1	3	4						
Fragilariopsis sublinearis				6	2						
Fragilariopsis linearis		2		2							
Fragilariopsis angulata											
Fragilariopsis cylindrus			3		5						
Fragilariopsis curta							1				
Fragilariopsis vanheurckii							1				
Fragilariopsis seriata											
Fragilariopsis ritscherii											
Fragilariopsis babieri											
Fragilariopsis pseudoanana											
Porosira glacialis				1							
Porosira pseudodenticulata											
Rhizosolenia simplex				2	2		1				
Rhizosolenia polydactila											
Rhizosolenia sp.											
Rhizosolenia hebetata											
Rhizosolenia setigera				2	2	2					
Rhizosolenia antennata											
Rhizosolenia (twin process) antennata											
Rhizosolenia inermis		1									
Rhizosolenia curvata											
Stellarima microtrias	2	5	16	5	2	2	1	0	0	0	0
Thalassiosira gracilis	2	1			3	1					
Thalassiosira lentiginosa	292	481	358	191	208	28	122	5	11	1	2
Thalassiosira oestrupii	2	7	3	4	2	2	3		1		
Thalassiosira oliverana	10	3	1	18	10	2	9	0	1	5	0
Thalassiosira ritscherii				1	1		2				
Thalassiosira tumida	11	10			4	1	4				
Thalassiotrix antarctica		3									
Thalassiothrix longisima		3									
Trichotoxon reinboldii		1									
Triceratium spp					1						1
Total counts	473	737	486	454	448	89	248	10	16	9	8

References

Blott, S. J. and Pye, K.: GRADISTAT: a grain size distribution and statistics package for the analysis of unconsolidated sediments, Earth surface processes and Landforms, 26, 11, 1237-1248, 2001.

Cook, C. P., van de Flierdt, T., Williams, T., Hemming, S. R., Iwai, M., Kobayashi, M., Jimenez-Espejo, F. J., Escutia, C., González, J. J., Khim, B. K., McKay, R. M., Passchier, S., Bohaty, S. M., Riesselman, C. R., Tauxe, L., Sugisaki, S., Galindo, A. L., Patterson, M. O., Sangiorgi, F., Pierce, E. L., Brinkhuis, H., Klaus, A., Fehr, A., Bendle, J. A. P., Bijl, P. K., Carr, S. A., Dunbar, R. B., Flores, J. A., Hayden, T. G., Katsuki, K., Kong, G. S., Nakai, M., Olney, M. P., Pekar, S. F., Pross, J., Röhl, U., Sakai, T., Shrivastava, P. K., Stickley, C. E., Tuo, S., Welsh, K. and Yamane, M.: Dynamic behaviour of the East Antarctic ice sheet during Pliocene warmth, Nature Geoscience, 6, 765, 2013.

Diekmann, B., Fütterer, D., Grobe, H., Hillenbrand, C., Kuhn, G., Michels, K., Petschick, R. and Pirrung, M.: Terrigenous sediment supply in the polar to temperate South Atlantic: Land-ocean links of environmental changes during the late Quaternary, in The South Atlantic in the Late Quaternary, Springer, 375-399, 2003.

Grobe, H. and Mackensen, A.: Late Quaternary climatic cycles as recorded in sediments from the Antarctic continental margin, The Antarctic Paleoenvironment: A Perspective on Global Change: Part One, 349-376, 1992.

Lisiecki, L. E. and Raymo, M. E.: A Pliocene-Pleistocene stack of 57 globally distributed benthic δ18O records, Paleoceanography, 20, 1, 2005.

Passchier, S.: Linkages between East Antarctic Ice Sheet extent and Southern Ocean temperatures based on a Pliocene high-resolution record of ice-rafted debris off Prydz Bay, East Antarctica, Paleoceanography, 26, 4, 2011.

Patterson, M. O., McKay, R., Naish, T., Escutia, C., Jimenez-Espejo, F. J., Raymo, M. E., Meyers, S. R., Tauxe, L., Brinkhuis, H., Klaus, A., Fehr, A., Bendle, J. A. P., Bijl, P. K., Bohaty, S. M., Carr, S. A., Dunbar, R. B., Flores, J. A., Gonzalez, J. J., Hayden, T. G., Iwai, M., Katsuki, K., Kong, G. S., Nakai, M., Olney, M. P., Passchier, S., Pekar, S. F., Pross, J., Riesselman, C. R., Röhl, U., Sakai, T., Shrivastava, P. K., Stickley, C. E., Sugasaki, S., Tuo, S., van de Flierdt, T., Welsh, K., Williams, T. and Yamane, M.: Orbital forcing of the East Antarctic ice sheet during the Pliocene and Early Pleistocene, Nature Geoscience, 7, 11, 841-847, 2014.

Pudsey, C. J. and Camerlenghi, A.: 'Glacial–interglacial deposition on a sediment drift on the Pacific margin of the Antarctic Peninsula, Antarctic Science, 10, 3, 286-308, 1998.

Williams, M.: *RV Tangaroa* Voyage Report Tan1302- Mertz Polynya Voyage 1 February to 14 March 2013, *NIWA, Wellington, New Zealand,* 19-33, 80, 2013.

Williams, G., Aoki, S., Jacobs, S., Rintoul, S., Tamura, T. and Bindoff, N.: Antarctic bottom water from the Adélie and George V Land coast, East Antarctica (140–149 E), Journal of Geophysical Research: Oceans, 115, C4, 2010.

Williams, G., Bindoff, N., Marsland, S. and Rintoul, S.: Formation and export of dense shelf water from the Adélie Depression, East Antarctica, Journal of Geophysical Research: Oceans, 113, C4, 2008.

Wilson, D. J., Bertram, R. A., Needham, E. F., van de Flierdt, T., Welsh, K. J., McKay, R. M., Mazumder, A., Riesselman, C. R., Jimenez-Espejo, F. J. and Escutia, C.: Ice loss from the East Antarctic Ice Sheet during late Pleistocene interglacials, Nature, 561, 7723, 383, 2018.